

**Biophysical Journal, Volume 114**

**Supplemental Information**

**K-Ras4B Remains Monomeric on Membranes over a Wide Range  
of Surface Densities and Lipid Compositions**

**Jean K. Chung, Young Kwang Lee, John-Paul Denson, William K. Gillette, Steven  
Alvarez, Andrew G. Stephen, and Jay T. Groves**

*Supporting Information for:*

**Membrane-reconstituted K-Ras4B remains monomeric over a wide range of surface densities and membrane lipid compositions**

**Contents**

A. Characterization of the full-length K-Ras .....	2
B. K-Ras equilibration to supported lipid bilayers.....	3
C. Experimental precision for FCS .....	4
D. Estimating diffusion coefficients for monomeric and dimeric Ras .....	5
E. Calculating FCS binding curve for two-dimensional dimerization reaction.....	6
F. Estimating 3-dimensional concentration from 2-dimensional surface density .....	9
G. Single molecule trajectory analysis .....	10

## A. Characterization of the full-length K-Ras

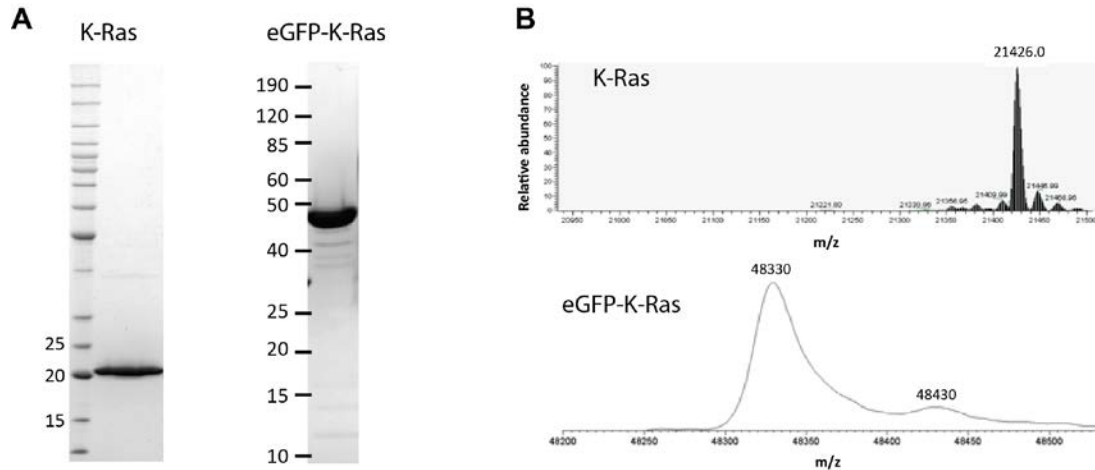


**Figure S1 Characterization of processed K-Ras and eGFP-K-Ras.** (A) SDS-PAGE analysis, (B) intact electrospray ionization mass spectrometry of the fully processed K-Ras4B constructs. The theoretical molecular weight of K-Ras4B and eGFP-KRas4B are 21426 and 48330 Da, respectively. The minor species observed at 48430 for eGFP-KRas4B is a 100 Da adduct formed during the liquid chromatography (LC) step prior to ESI-MS analysis. This species is not present when the sample is directly injected for ESI-MS analysis, bypassing the LC system.

The amino acid sequence for K-Ras4B after processing, including the farnesylation and methylation is:

**GGSG**TEYKLVVVGAGGVGKSALTIQLIQNHVDEYDPTIEDSYRKQVVIDGETCLLDILDITAGQEEYSAMRDQYMRTGE  
GFLCVFAINNTKSFEDIHHYREQIKRVKDESDVPMVLVGNKCDLPSRTVDTKQAQDLARSYGIPFIETSAKTRQGVDFAF  
YTLVREIRKHKEKMSKDGGKKKKKSKTKC-FMe

The residues remaining after TEV cleavage are shown in red. The underlined Thr is the first amino acid in the K-Ras4B sequence. The final molecular weight is 21426 Da.

For eGFP-labeled K-Ras, the final amino acid sequence is:

GMVSKGEELFTGVVPIVVELDGDVNGHKFSVSGEGEGDATYGKLT~~LKFICTTGKLPVPWPTLVTTLTYGVQCFSRYPDH~~  
MKQHDFFKSAMPEGYVQERTIFFKDDGNYKTRAEVKFEGDTLVNRIELKGIDFKEDGNILGHKLEYNYNHNVYIMADK  
QKNGIKVNFKIRHNIEDGSVQLADHYQQNTPIGDGPVLLPDNHYLSTQSALSQDPNEKRDHMLLEFVTAAGITLGM  
ELYK**GGSG**TEYKLVVVGAGGVGKSALTIQLIQNHVDEYDPTIEDSYRKQVVIDGETCLLDILDITAGQEEYSAMRDQYMRT  
GEGFLCVFAINNTKSFEDIHHYREQIKRVKDESDVPMVLVGNKCDLPSRTVDTKQAQDLARSYGIPFIETSAKTRQGVD  
AFYTLVREIRKHKEKMSKDGGKKKKKSKTKC-FMe

The linker sequence is shown in red. The final molecular weight for this construct after farnesylation and methylation is 48330 Da.

## B. K-Ras equilibration to supported lipid bilayers

Upon introduction to supported lipid bilayer, K-Ras spontaneously inserts itself to the membrane and reaches stable equilibrium in ~10 minutes. The membrane binding kinetics showed no difference between GDP- and GTP-bound states.

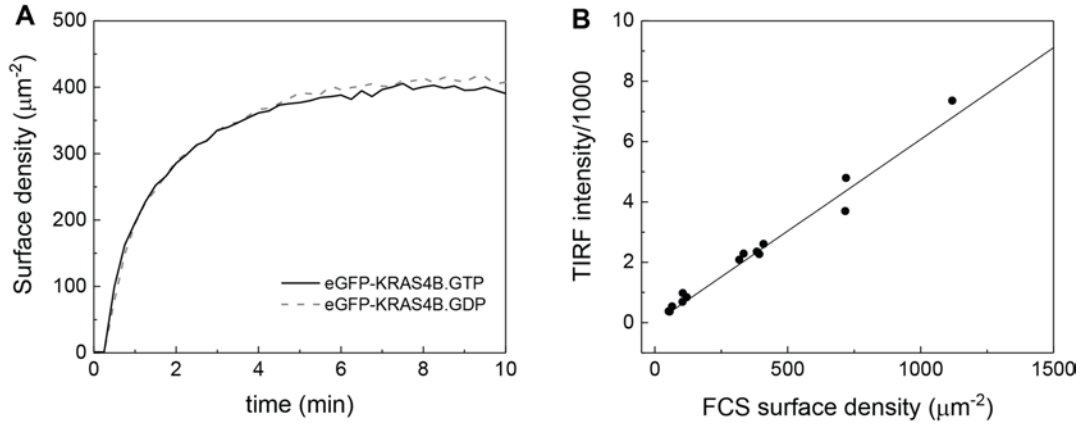


**Figure S2 Spontaneous insertion of eGFP-labeled K-Ras4B onto supported lipid bilayer.** **A** The adsorption of 40 nM GTP- and GDP-bound K-Ras onto 10% PS bilayer, monitored by TIRF microscopy. **B** The TIRF intensity was calibrated to the surface density of eGFP-KRas4B by correlating FCS surface density measurements to the TIRF intensity. Within the experimental range, the TIRF intensity increased linearly with the number of K-Ras on the membrane surface.

### C. Experimental precision for FCS

Here, we will discuss the experimental precision for the FCS measurements on supported lipid bilayers. For each sample condition, four spots in the SLB's are measured, at least 1  $\mu\text{m}$  apart from each other. Each autocorrelation trace is average of 10 scans of 5 seconds. Shown below are autocorrelation data obtained from low-density eGFP-KRas4B.GTP:

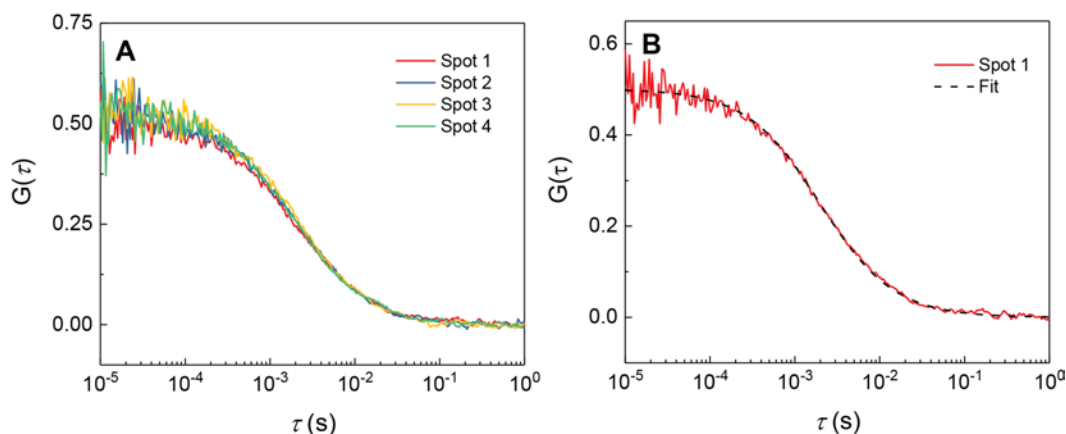


**Figure S3** FCS experimental precision. **A** Ten 5-scan averages were collected for four spots in the supported lipid bilayer sample. **B** Autocorrelation data from Spot 1 was fit to Equation 1.

Autocorrelation functions collected from four spots in the sample are displayed in Figure S2A. Then, each autocorrelation function is fit to 2D Gaussian diffusion model, Equation 1, shown in Figure S2B, and the residence time  $\tau_d$  and  $N$  are obtained. The table below summarizes fit values from each autocorrelation function.

Spot	$\tau_d$ (ms)	$N$
1	1.97	2.00
2	1.91	1.91
3	1.93	1.86
4	1.85	1.88
Average	1.91	1.91
Standard error	0.025	0.030

For this set of measurements, the standard error for the fit values were less than 2% for both  $\tau_d$  and  $N$ . Each data point shown in FCS measurements such as Figure 2A represent the average of 3-4 spots such as these. The standard error was no more than 5% for all of data presented in this work. The scatter in the data may reflect actual heterogeneities in the bilayer samples, which could have had uneven areas in the glass substrates, on top of some day-to-day variations.

#### D. Estimating diffusion coefficients for monomeric and dimeric Ras

To determine the diffusion coefficients for Ras monomers and dimers, we titrated Ras surface density in excess RBD-LeuZ crosslinker, and examined the changing diffusion rates. At very low Ras density, the diffusion coefficient was approximately  $4.5 \mu\text{m}^2/\text{s}$ , which is same as Ras without the crosslinker—therefore, this is the diffusion coefficient of Ras monomer. Then, as Ras surface density increases, diffusion decreases crosslinked species begin to appear.

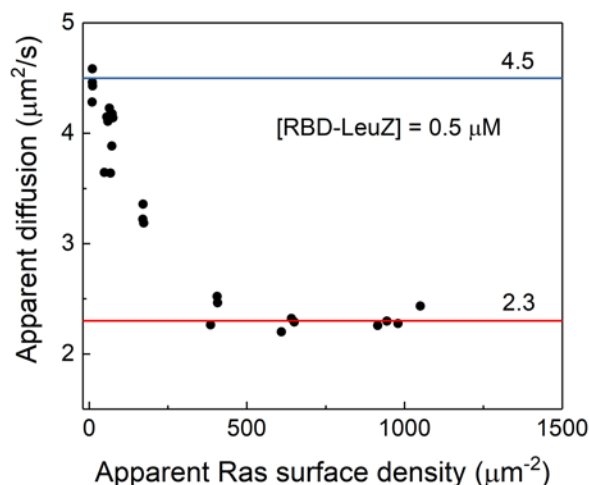


**Figure S4** FCS diffusion measurement for monomeric and dimeric Ras using RBD-LeuZ crosslinker.

As the apparent density approaches the detection limit ( $\sim 1500 \mu\text{m}^2$ ), the diffusion coefficient value is observed to plateau near  $2.3 \mu\text{m}^2/\text{s}$ . In principle, it is unknown whether all Ras are dimeric at this point, as the dimer fraction for this crosslinking reaction is convolution of the binding affinities between Ras:RBD and LeuZ:LeuZ. Presumably, there is a regime of Ras surface density and RBD-LeuZ concentration where all Ras are crosslinked, but it is unknown whether these experimental conditions are within that zone. Still,  $2.3 \mu\text{m}^2/\text{s}$  provides a reasonable approximation, and it is close to the decreased diffusion value by dimerization observed in other systems (41). Furthermore, since this is an upper limit for the true diffusion coefficient of the dimer, all calculations performed with this value generally resulted in conservative estimates in differentiating dimers from monomers.

## E. Calculating FCS binding curve for two-dimensional dimerization reaction

In this section, theoretical FCS diffusion measurements for two-dimensional dimerization reactions with arbitrary dissociation constants will be discussed. These are details pertaining to Figure 2 in the main text. Because both molecular brightness and diffusion change due to dimerization, its effect on the shape of the binding curve is not straightforward.

As discussed in the text, Ras dimerization on a membrane surface can be considered as a simple bimolecular reaction,



Then, the two-dimensional dissociation constant  $K_d$  is defined as

$$K_d = [Ras]^2 / [Ras \cdot Ras] \quad (S2)$$

Where  $[Ras]$  and  $[Ras \cdot Ras]$  denote the two-dimensional surface density for monomers and dimers, respectively. For simplicity's sake, let us denote the surface density of monomers, dimers, and total Ras molecules as  $X_m$ ,  $X_d$ , and  $X$ , respectively, such that  $X = X_m + 2X_d$ . The surface density of dimers  $X_d$  as a function of surface density  $X$  is given by

$$X_d = \frac{1}{8} \left( K_d + 4X - \sqrt{K_d(K_d + 8X)} \right) \quad (S3)$$

The derivation for this expression can be found in (11). For a hypothetical dimerization reaction with  $K_d = 200 \mu\text{m}^{-2}$ , the theoretical “binding curve” can be visualized as follows:

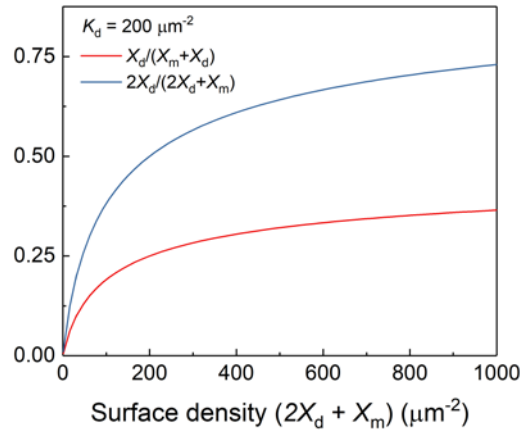


**Figure S5** Calculated dimer fractions from Equation S3 for  $K_d = 200 \mu\text{m}^{-2}$ .

Here, we make the distinction between two types of dimer fractions: *numerical* dimer fraction,  $X_d/(X_d + X_m)$ , and *chemical* dimer fraction,  $2X_d/(2X_d + X_m)$ . While the chemical dimer fraction is the quantity of interest for the dimerization reaction, numerical dimer fraction is more directly relevant to the FCS observables, as the  $N$  value obtained from FCS is sensitive (for the most part) only to the number of diffusing particles regardless of their identity.

For a sample with two different molecular brightness  $B_1$  and  $B_2$ , and two-dimensional Gaussian focus residence time of  $\tau_1$  and  $\tau_2$ , the autocorrelation function  $G(\tau)$  is given by:

$$G(\tau) = \frac{N_1 B_1^2 (1 + \tau/\tau_1)^{-1} + N_2 B_2^2 (1 + \tau/\tau_2)^{-1}}{(N_1 B_1 + N_2 B_2)^2} \quad (\text{S4})$$

Where  $N$ ,  $B$ ,  $\tau$ , are number of particles, molecular brightness, and focus residence time, respectively (33). This equation is a form of Equation 5 for two components. One consequence of this relation is that the autocorrelation is strongly weighted by the brighter species in the sample. Let us consider a hypothetical mixture of monomers and dimers, with  $B_1 = 1$ ,  $B_2 = 2$ ,  $D_1 = 4.5 \mu\text{m}^2/\text{s}$ , and  $D_2 = 2.3 \mu\text{m}^2/\text{s}$ , where the subscripts 1 and 2 correspond to monomers and dimers, for a spot size of  $w = 200 \text{ nm}$ . Then,  $G(\tau)$  for purely monomeric (red), purely dimeric (blue), and equal population of monomers and dimers (broken green line) can be calculated using Equation S4:

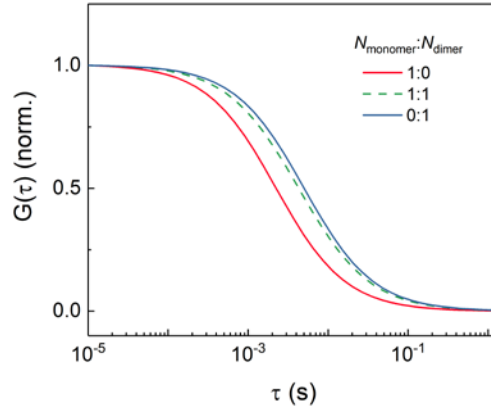


**Figure S6** Calculated FCS autocorrelation for mixed populations.

Due to the brightness effect, the autocorrelation for 1:1 mixture is clearly not the average of the monomers and dimers, but is much closer to the autocorrelation function for the purely dimeric population, because the slower and twice-brighter dimers are much more strongly represented. Fitting this autocorrelation to a single-species model, Equation 1, yields:

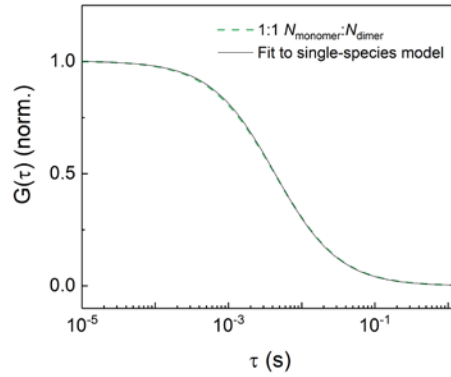


**Figure S7** Single-species fitting to mixed population autocorrelation function.

Even with the calculated, noiseless two-population  $G(\tau)$ , the single species model fit is nearly perfect: this due to the gently sloping lineshape of the FCS autocorrelation function. The apparent diffusion coefficient from this fit is  $2.6 \mu\text{m}^2/\text{s}$ .

By performing same simulations for each particle density, we can calculate a theoretical FCS experiment. Note that this is not an analytical calculation, because there is no analytical solution for 1-species model (Equation 1) for two-species autocorrelation function (Equation S4). Therefore, this calculation is a numerical estimation based on optimization.

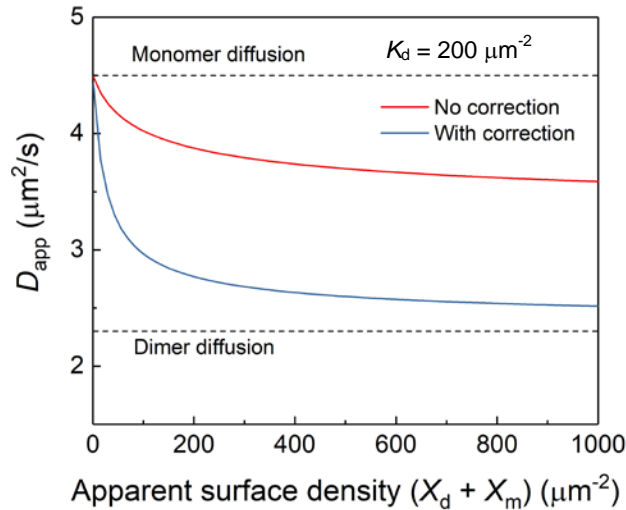


**Figure S8** Simulated FCS binding curve with the brightness effect correction.

Here, the apparent diffusion coefficient for two-species autocorrelation function are shown in (blue). This is contrasted to the case in which there is no nonlinear contribution from unequal molecular brightness (*i.e.* if  $B_1 = B_2$ ). This comparison highlights the fact that dimers are much more readily detected in an FCS experiment than would be otherwise, giving it a wide effective dynamic range. Note that for the  $x$ -axis for this calculated experiment is *apparent* surface density  $X_d + X_m$  as would have been obtained from the FCS autocorrelation function. For Figure 2B in the main text, same calculations were performed for a series of  $K_d$  values.

## F. Estimating 3-dimensional concentration from 2-dimensional surface density

Here, we will outline how three-dimensional concentration from two-dimensional surface density may be estimated. More details can be found in (11). The translational entropy, or the entropy of mixing, is determined only by the fractional occupation. In other words,

% occupied volume in 3D = % occupied area in 2D

For Ras in solution, the unit volume encasing the protein is approximately 3 nm-cube, and the equivalent area on membranes is a 3 nm-square. Then, for surface density of  $x \mu\text{m}^{-2}$ , the fraction of occupied area is

$$(3 \text{ nm})^2 \times x \mu\text{m}^{-2} \times (1 \mu\text{m}^2 / 10^6 \text{ nm}^2) = (9 \times 10^{-6})x$$

For one liter, the volume occupied by Ras is

$$1 \text{ L} \times (9 \times 10^{-6})x \times (10^{24} \text{ nm}^3 / 1\text{L}) = (9 \times 10^{18})x \text{ nm}^3$$

And the number of Ras in this volume is

$$(9 \times 10^{18})x \text{ nm}^3 \times \frac{1 \text{ Ras}}{(3 \text{ nm})^3} \times \frac{1 \text{ mol}}{6.022 \times 10^{23} \text{ Ras}} = (6 \times 10^{-7})x \text{ mol}$$

Therefore, for Ras, two-dimensional surface density  $x \mu\text{m}^{-2}$  is equivalent to  $0.6 x \mu\text{M}$ .

## G. Single molecule trajectory analysis

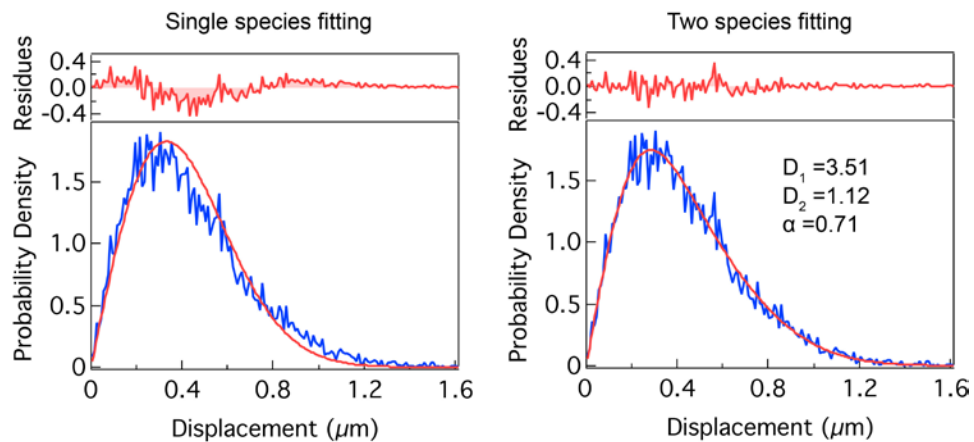


**Figure S9.** A single and two species fitting of step size distribution of K-Ras. A single species model (Equation 3 with  $\alpha = 1$ ) yields systematic fitting residues and fails to describe the step size distribution. However, two species model (Equation 3) adequately describe the distribution. The distribution was acquired with 100 pM K-Ras labeled with GppNHp-AF647 on a 20% DOPS and 80% DOPC membrane at 20 ms frame rate.